Flux Emissivity Tables for Water Vapor, Carbon Dioxide and Ozone

D. O. STALEY AND G. M. JURICA[1]

Institute of Atmospheric Physics, The University of Arizona, Tucson

(Manuscript received 16 December 1969)

ABSTRACT

Flux emissivities for the H_2O bands and window, and for CO_2 and O_3, were evaluated from Elsasser's wavelength-dependent absorption coefficients and flux transmissivities. The flux emissivities for water vapor differ significantly from previously published emissivities based on Elsasser's incorrect flux densities. A flux emissivity correction for the overlap of H_2O and CO_2 is defined and evaluated for combinations of optical depths.

The largest partial emissivity is associated with the H_2O rotation band, and it increases markedly with decreasing temperature, while the partial emissivities associated with the 6.3 μ band and the window are smaller and decrease with decreasing temperature. Emissivity in the window increases very rapidly with optical depths $\gtrsim$ 1 gm cm^{-2}. The total H_2O flux emissivity is remarkably independent of temperature, especially in the range from -40 to 20C, as a result of near cancellation of the temperature dependences in three regions of the spectrum. The total flux emissivity increases rapidly with optical depth beyond $\sim$1 gm cm^{-2} as a result of emission in the window. An H_2O column with a temperature of 20C is 98% black for optical depths $>$50 gm cm^{-2}.

The flux emissivity of CO_2 increases slightly with temperature at all but the very smallest optical depths. This result traces physically to the increase of absorption with temperature at the edges of the 15 μ band.

The correction to flux emissivity resulting from the overlap of H_2O and CO_2 radiation is negative and increases markedly with the optical depths of both. It is of the order of -0.05 to -0.10 for typical total atmospheric optical depths. This emissivity correction for overlap shows a large percentage increase with temperature, principally as a result of increasing absorption with temperature in the wings of both the rotation band of H_2O and the 15 μ CO_2 band.

The flux emissivity of O_3 undergoes a large percentage decrease with temperature. For typical total O_3 depths, the emissivity for -70C is less than half its value at 20C.

1. Introduction

The purpose of this paper is to present flux emissivities for homogeneous slabs of H_2O, CO_2 and O_3, with a correction to emissivity for the overlap of H_2O and CO_2. The computations utilize Elsasser and Culbertson's (1960) wavelength-dependent generalized absorption coefficients and flux transmissivities, but do not utilize their quantity $R(u,T)$. Zdunkowski *et al.* (1966) have shown that because of an incorrect integration the quantity R as tabulated by Elsasser and Culbertson cannot be used to calculate flux densities. It follows that emissivities presented by Fleagle and Businger (1963) and by Sellers (1965) on the basis of the Elsasser and Culbertson tabulations cannot be correct.

Zdunkowski *et al.* tabulate corrected tables of $R(u,T)$ for CO_2 and the total H_2O spectrum, but they do not tabulate for individual H_2O bands. They indicate the need for separate H_2O-CO_2 overlap tables for different temperatures but give only a few examples for some reasonable combinations of temperature and optical depths. They do not treat ozone.

The present tabulations differ from and extend the work of Zdunkowski *et al.* in the following ways: Computations are made in terms of the flux emissivity of a slab homogeneous in temperature and pressure, and for the separate bands of H_2O. Computations are made for O_3. The correction for overlap of H_2O and CO_2 is defined differently from Elsasser and Culbertson and Zdunkowski *et al.*, and tabulations are presented for -70, -40, -10 and 20C over the complete ranges of CO_2 and H_2O optical depths for which Elsasser and Culbertson presented absorption data.

The computations were made in all cases from Elsasser and Culbertson's original wavelength- and temperature-dependent generalized absorption coefficients and flux transmissivities, none from the tabulations of corrected $R(u,T)$ given by Zdunkowski *et al.* However, where corresponding flux densities could be obtained from their tabulations, division by the blackbody flux density yielded emissivities in good agreement with the present results. The correctness of our interpretation of Elsasser and Culbertson's treatment of the absorption data was also checked by direct calculation of selected values of their $R(u,T)$. Good agreement was found with tabulations in both of the foregoing papers. The small discrepancies probably trace to slight

[1] Present affiliation: Department of Geosciences, Purdue University, Lafayette, Ind.

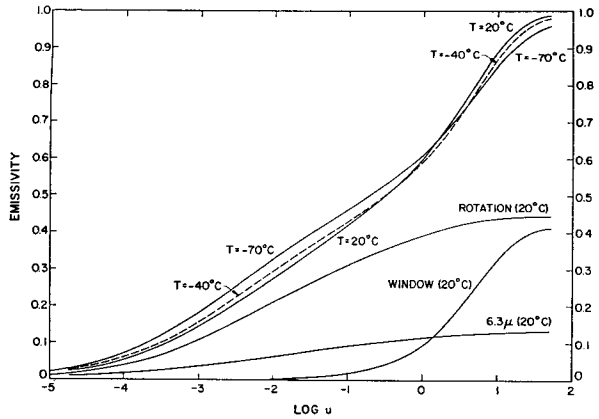

FIG. 1. H_2O emissivity as a function of optical depth (pressure-corrected gm cm^{-2}) for $T=20$, -40, -70C, and the contributions of the rotation band, 6.3 μ band, and window for $T=20$C.

differences of wavenumber limits and the accuracy to which necessary data can be extracted from the Elsasser monograph.

The wavelength-dependent generalized absorption coefficients and flux transmissivities presented by Elsasser and Culbertson should indeed be questioned, and some critical comments will be made in the conclusion to this paper. However, computations of flux densities and cooling rates based on the Elsasser monograph are widespread, and comparisons are being made with computations based on other work or with observations. The detailed emissivities presented here should facilitate location of discrepancies in the basic absorption data or their subsequent treatment in various methods of computation.

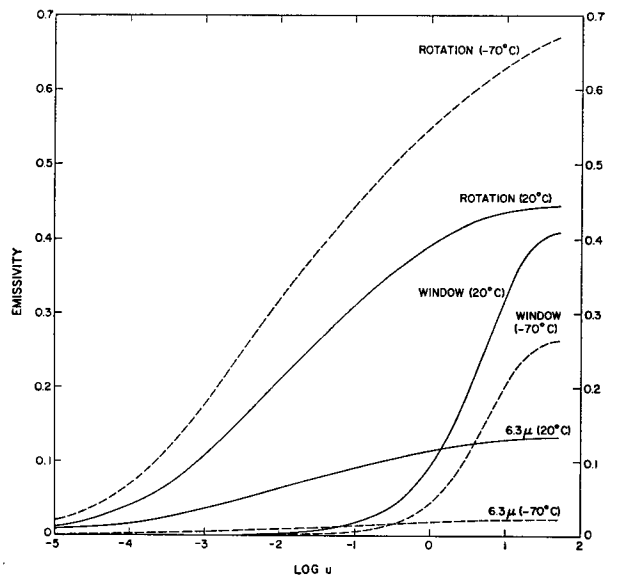

FIG. 2. Contributions of the rotation band, 6.3 μ band, and window to H_2O emissivity at 20 and at -70C.

2. Emissivities

The emission of O_3 is small compared with, and does not significantly overlap, emission of H_2O and CO_2. We may therefore deal with H_2O and CO_2, independently of O_3. The flux emissivity for a combination of H_2O and CO_2 may be written as

$$\epsilon(u,h,T)=\int_0^\infty B(n,T)[1-\tau_F(n,u,T)\tau_F(n,h,T)]dn \Big/ \int_0^\infty B(n,T)dn, \quad (1)$$

where u and h are optical depths of H_2O and CO_2, respectively, $B(n,T)$ is Planck's law in terms of flux per wavenumber n, and $\tau_F(n,u,T)$, $\tau_F(n,h,T)$ are the laboratory flux transmissivities of H_2O and CO_2, respectively. The denominator is simply σT^4, and, by rearrangement of the numerator, we can write

$$\epsilon(u,h,T)=\underbrace{\frac{\int_0^\infty B(n,T)[1-\tau_F(n,u,T)]dn}{\sigma T^4}}_{\epsilon(u,T)} + \underbrace{\frac{\int_0^\infty B(n,T)[1-\tau_F(n,h,T)]dn}{\sigma T^4}}_{\epsilon(h,T)} - \underbrace{\frac{\int_0^\infty B(n,T)[1-\tau_F(n,u,T)][1-\tau_F(n,h,T)]dn}{\sigma T^4}}_{\Delta\epsilon(u,h,T)}. \quad (2)$$

The first two terms can be identified as the emissivities of H_2O and CO_2, respectively, while the final term can be identified as a correction to $\epsilon(u,h,T)$ for overlap of the wings of H_2O and CO_2 radiation. $\Delta\epsilon(u,h,T)$ is a positive quantity which must be subtracted from the first two terms in order to give the correct emissivity. The overlap correction quantity, $\Delta\epsilon$, is not analogous to Elsasser and Culbertson's overlap correction, $-\Delta R$, or to the corrected correction, $-\Delta R^*$, defined by Zdunkowski *et al.* After treating H_2O as if CO_2 were not present, they note that, instead of $\tau_F(H_2O)$, the transmissivity should be written as $\tau_F(H_2O)\tau_F(CO_2)$ in the region of overlap. They are led to an overlap correction which includes R_{CO_2} as well as a term analogous to the quantity $\Delta\epsilon$ in (2). In our opinion, the formulation in (1) and (2) is preferable from the standpoint of physical insight.

TABLE 1. Flux emissivities for H_2O (percent).

	Rotation				Window				6.3 μ				Total			
Log u	−70C	−40C	−10C	20C	−70C	−40C	−10C	20C	−70C	−40C	−10C	20C	−70C	−40C	−10C	20C
−5.0	2.02	1.57	1.28	1.08	0.00	0.00	0.00	0.00	0.14	0.32	0.58	0.88	2.16	1.90	1.86	1.96
−4.7	3.01	2.38	1.96	1.66	0.00	0.00	0.00	0.00	0.15	0.34	0.62	0.95	3.16	2.72	2.58	2.62
−4.3	4.92	3.94	3.27	2.79	0.00	0.00	0.00	0.00	0.20	0.46	0.84	1.30	5.11	4.40	4.11	4.09
−4.0	6.91	5.57	4.65	3.98	0.00	0.00	0.00	0.00	0.25	0.59	1.07	1.67	7.16	6.16	5.72	5.65
−3.7	9.45	7.66	6.44	5.54	0.00	0.00	0.00	0.00	0.31	0.75	1.37	2.13	9.77	8.41	7.81	7.68
−3.3	13.7	11.2	9.52	8.25	0.00	0.00	0.00	0.00	0.42	1.00	1.85	2.90	14.1	12.2	11.4	11.2
−3.0	17.5	14.5	12.3	10.7	0.01	0.01	0.01	0.01	0.51	1.23	2.27	3.58	18.0	15.7	14.6	14.3
−2.7	21.7	18.1	15.5	13.6	0.01	0.01	0.01	0.02	0.62	1.48	2.75	4.34	22.3	19.6	18.3	18.0
−2.3	27.5	23.2	20.2	17.8	0.03	0.03	0.04	0.07	0.76	1.83	3.41	5.42	28.3	25.1	23.6	23.2
−2.0	31.7	27.1	23.7	20.9	0.05	0.06	0.09	0.18	0.86	2.08	3.90	6.21	32.6	29.2	27.7	27.3
−1.7	35.7	30.8	27.2	24.1	0.10	0.13	0.21	0.41	0.98	2.37	4.46	7.10	36.8	33.3	31.9	31.6
−1.3	40.8	35.6	31.7	28.1	0.26	0.34	0.57	0.96	1.14	2.76	5.18	8.24	42.2	38.8	37.4	37.3
−1.0	44.4	39.1	34.9	31.0	0.51	0.70	1.10	1.69	1.26	3.04	5.69	9.03	46.2	42.8	41.7	41.8
−0.7	47.8	42.4	37.9	33.8	1.01	1.40	2.04	2.89	1.39	3.32	6.19	9.79	50.2	47.1	46.2	46.5
−0.3	52.0	46.4	41.6	37.1	2.43	3.29	4.40	5.72	1.56	3.68	6.83	10.7	56.0	53.4	52.9	53.6
0.0	54.9	49.2	44.2	39.2	4.49	5.94	7.57	9.34	1.69	3.96	7.30	11.4	61.1	59.1	59.0	60.0
0.3	57.6	51.8	46.4	41.0	7.86	10.2	12.5	14.7	1.82	4.22	7.72	12.0	67.3	66.2	66.6	67.7
0.7	60.8	54.7	48.8	42.8	14.6	18.5	21.8	24.5	1.98	4.52	8.18	12.6	77.4	77.8	78.8	79.8
1.0	63.0	56.6	50.1	43.6	20.2	25.5	29.5	32.4	2.09	4.72	8.45	12.9	85.3	86.8	88.1	88.8
1.3	65.0	58.1	51.1	44.1	24.4	30.8	35.3	38.2	2.19	4.89	8.64	13.1	91.5	93.8	95.1	95.4
1.7	67.1	59.6	51.8	44.4	26.3	33.3	38.2	41.0	2.30	5.05	8.81	13.2	95.8	98.0	98.8	98.7

3. Water vapor emissivities

Figs. 1 and 2 and Table 1 show the partial emissivities of the rotation band, window, and 6.3 μ band. In Fig. 1 these are shown for 20C. The largest contribution to total emissivity is made by the rotation band. The contribution in the window is very small at the shorter optical depths, but increases rapidly with optical depth for $u \gtrsim 0.5$ gm cm^{-2}, and exceeds the 6.3 μ band contribution for $u \gtrsim 1.4$ gm cm^{-2}. At very large optical depths, of course, all three regions become perfectly absorbing, and the three partial emissivities approach asymptotes representing the proportion of σT^4 in each spectral region. The rapid rise in the total emissivity curve at large optical depths may be recognized as resulting from the rapidly increasing contribution from the window region.

In the tables presented in this paper, three significant figures are given for the larger emissivities, but the final figure is possibly inaccurate. In any event, the significant figures reflect only the sort of accuracy with which the various quantities necessary to the computations can be obtained from Elsasser's monograph; more recent absorption data, or other equally justifiable treatments of the data, may lead to substantially different emissivities.

Fig. 2 shows the variation with temperature of the partial emissivities. As temperature is decreased to −70C, the contribution of the rotation band becomes even more dominant, while the window region contributes less and the contribution of the 6.3 μ band becomes almost negligible. The window region contributes more than the 6.3 μ band for $u > 0.3$ gm cm^{-2}.

The total emissivity shows less variability with temperature than do the partial contributions of the rotation and 6.3 μ bands. The nearly equal and opposite variations with temperature of these two bands is fortuitous but does not necessarily imply that the total emissivity may be used safely to calculate the H_2O flux density in an atmosphere with a temperature gradient.

The relationship between $\epsilon(u,T)$, as calculated here from Elsasser and Culbertson's absorption coefficients and flux transmissivities, and $\epsilon'(u,T)$, as calculated from their $R(u,T)$, is shown in Fig. 3. It is seen that the erroneous ϵ' seriously underestimates ϵ. The downward flux density of H_2O radiation from an isothermal atmosphere at 20C with an optical depth of 1 gm cm^{-2} would be underestimated by 12% if ϵ' were used instead of ϵ. This value compares well with the finding by Zdunkowski *et al.* of errors in the range from 8–18% in the flux densities from isothermal layers.

Slopes of the emissivity curve presented by Fleagle and Businger (1963) appear to be in even more serious error than the emissivities themselves. They propose

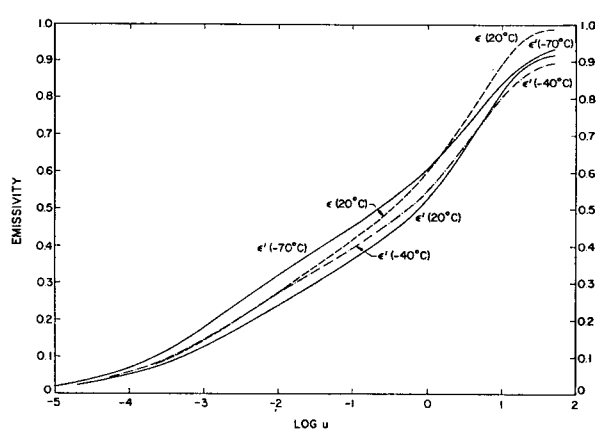

FIG. 3. Incorrect emissivity ϵ' for H_2O as a function of optical depth for $T = 20$, −10, −40 and −70C, in comparison with the correct emissivity ϵ, for $T = 20$C.

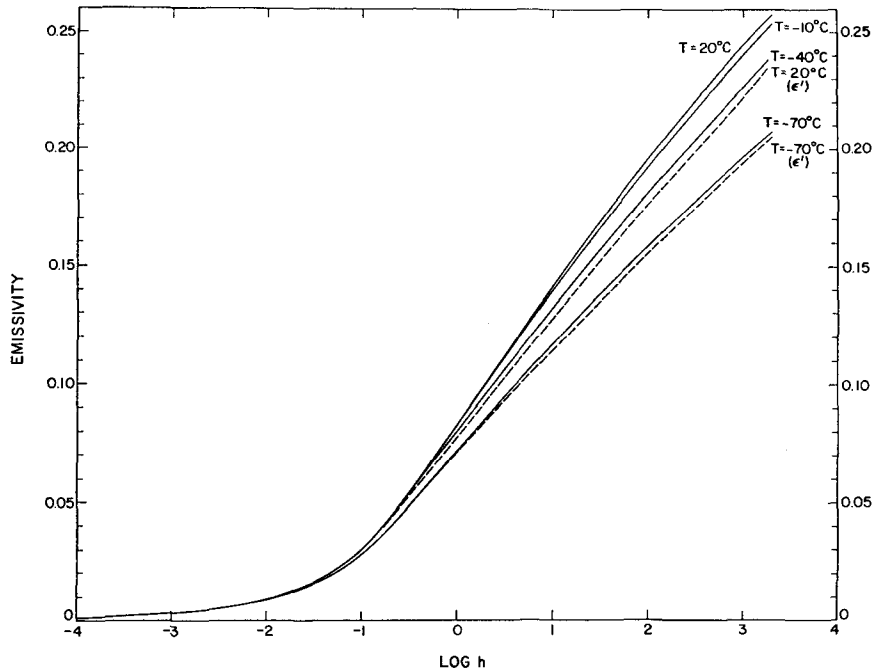

FIG. 4. CO_2 emissivity as a function of optical depth (pressure-corrected cm at STP) for $T=20$, -10, -40, -70C, and the incorrect emissivity ϵ' for $T=20$ and -70C.

that downward flux density be evaluated from

$$F_{\downarrow}=\int_0^{u_T}\sigma T^4\gamma\,du, \tag{3}$$

where u_T is the value of optical depth corresponding to the top of the H_2O atmosphere, and $\gamma=\partial\epsilon(u,T)/\partial u$ is the rate of change of emissivity with optical depth at a fixed temperature. They present a "detailed" graph (their Fig. 4.17) of the relationship of γ to u for $T=-30$ and 10C. Although the curves appear close to each other, suggesting only a small dependence of slope on temperature, the scale is logarithmic, and the values of γ are substantially different for the same optical depth. In the range of optical depth from 10^{-5} to 10 gm cm^{-2}, the ratio $\gamma(10\text{C})/\gamma(-30\text{C})$ departs little from 1.4. Fleagle and Businger do not comment on this astonishingly large dependence of γ on temperature, but the implication is clear—flux density errors of up to 40%, or more, could occur, depending on what temperature is used to choose γ. Alternatively, great difficulties would be encountered in handling accurately the computation of flux density from an atmosphere with a temperature gradient. The curve of $\gamma(u,-30\text{C})$ presented by Fleagle and Businger cannot be obtained, even approximately, from either ϵ or ϵ' values in Table 1 and Fig. 1; it appears to be the result of unknown errors of catastrophic magnitude.

TABLE 2. Flux emissivities for CO_2 (percent).

Log h	−70C	−40C	−10C	20C
−4.0	0.114	0.119	0.115	0.108
−3.7	0.162	0.171	0.167	0.158
−3.3	0.247	0.262	0.260	0.248
−3.0	0.331	0.354	0.352	0.338
−2.7	0.439	0.471	0.471	0.454
−2.3	0.641	0.691	0.693	0.672
−2.0	0.859	0.928	0.934	0.907
−1.7	1.19	1.29	1.30	1.27
−1.3	1.92	2.08	2.11	2.07
−1.0	2.78	3.03	3.08	3.03
−0.7	3.92	4.30	4.39	4.32
−0.3	5.76	6.36	6.54	6.49
0.0	7.19	7.99	8.26	8.23
0.3	8.60	9.61	10.0	10.0
0.7	10.4	11.7	12.3	12.4
1.0	11.7	13.3	13.9	14.1
1.3	13.0	14.8	15.6	15.8
1.7	14.7	16.7	17.7	18.0
2.0	15.9	18.1	19.3	19.6
2.3	17.0	19.5	20.7	21.1
2.7	18.6	21.3	22.7	23.1
3.0	19.7	22.6	24.1	24.4
3.3	20.7	23.9	25.4	25.7

The determination of an accurate slope is difficult enough, and the determination of a mean slope, as seemingly required in the numerical evaluation of (3), is even more difficult. The limiting slope at zero optical depth is especially difficult to measure. There is, in fact, no necessity of dealing with forms involving γ. One recognizes that $\gamma du=d\epsilon$ and evaluates the flux density from $\int\sigma T^4 d\epsilon$ by relating temperature and emissivity to optical distance from the reference level. It is impossible to achieve the same accuracy by trying to use explicit values of γ directly in (3).

Brooks (1950) and Fleagle and Businger also give expressions for cooling rates which seem to require detailed values of γ, but here again, except at an optical

TABLE 3. H_2O-CO_2 overlap correction quantity, $\Delta\epsilon$, for −70C. To obtain $\Delta\epsilon$, multiply values in table by 10^{-4}.

	Log u															
Log h	−3.7	−3.3	−3.0	−2.7	−2.3	−2.0	−1.7	−1.3	−1.0	−0.7	−0.3	0.0	0.3	0.7	1.0	1.3	1.7
−4.0	0	0	0	0	0	0	0	0	0	1	1	2	4	6	8	9	10
−3.7	0	0	0	0	0	0	0	0	0	1	2	3	5	9	11	12	13
−3.3	0	0	0	0	0	0	0	0	1	1	3	5	8	13	17	19	20
−3.0	0	0	0	0	0	0	0	0	1	2	4	7	11	18	22	25	27
−2.7	0	0	0	0	0	0	0	0	1	2	5	9	14	24	30	33	36
−2.3	0	0	0	0	0	0	0	1	2	3	7	13	21	34	43	48	52
−2.0	0	0	0	0	0	0	0	1	2	4	10	17	28	46	58	65	70
−1.7	0	0	0	0	0	0	0	1	3	6	14	24	39	63	80	90	97
−1.3	0	0	0	0	0	0	1	2	5	9	22	38	62	101	128	144	156
−1.0	0	0	0	0	0	1	1	3	7	14	31	55	89	146	184	208	226
−0.7	0	0	0	0	0	1	2	4	10	19	44	77	124	204	258	292	319
−0.3	0	0	0	0	1	1	2	7	14	28	64	111	180	297	376	426	467
0.0	0	0	0	0	1	1	3	8	17	35	80	137	222	366	465	528	581
0.3	0	0	0	0	1	2	3	10	21	41	94	162	262	432	550	628	692
0.7	0	0	0	0	1	2	4	12	25	50	113	193	312	516	659	755	834
1.0	0	0	0	0	1	2	5	14	29	56	126	215	347	576	737	845	935
1.3	0	0	0	0	1	2	5	16	33	63	140	238	384	637	818	939	1040
1.7	0	0	0	0	1	3	6	19	38	72	158	268	432	717	922	1060	1180
2.0	0	0	0	0	1	3	7	21	42	80	172	290	466	774	997	1150	1280
2.3	0	0	0	1	1	3	8	24	47	87	186	313	501	831	1070	1240	1380
2.7	0	0	0	1	1	3	9	27	53	98	206	343	547	907	1170	1360	1520
3.0	0	0	0	1	2	4	10	30	58	106	220	366	582	964	1250	1450	1620
3.3	0	0	0	1	2	4	11	32	63	113	234	388	615	1020	1320	1540	1720

depth corresponding to the upper boundary of the atmosphere where its numerical value is not crucial, the integration can be carried out over emissivity itself.

4. Carbon dioxide emissivity

The results are shown in Table 2 and Fig. 4. The principal feature deserving comment is the increase of emissivity with temperature at all but the very smallest optical depths. This result traces physically to the increase of absorption with temperature at the edges of the 15 μ CO_2 band. This effect dominates the opposite effect at the center of the band, where absorption is already complete at very short optical depths. The variability in the fraction of the total blackbody energy contained in the 15 μ band is very small for temperatures in the range from 200–300K. Values of ϵ' at −70 and 20C are also shown in Fig. 4. As in the case of H_2O, ϵ' is an underestimate of ϵ.

5. Water vapor-carbon dioxide overlap

Since $\Delta\epsilon$ depends on u,h,T, the results cannot be represented on a single diagram as can the partial

TABLE 4. H_2O-CO_2 overlap correction quantity, $\Delta\epsilon$, for −40C. To obtain $\Delta\epsilon$, multiply values in table by 10^{-4}.

	Log u															
Log h	−3.7	−3.3	−3.0	−2.7	−2.3	−2.0	−1.7	−1.3	−1.0	−0.7	−0.3	0.0	0.3	0.7	1.0	1.3	1.7
−4.0	0	0	0	0	0	0	0	0	1	1	2	3	5	8	9	10	11
−3.7	0	0	0	0	0	0	0	0	1	1	3	5	7	11	13	15	16
−3.3	0	0	0	0	0	0	0	1	1	2	4	7	11	17	20	23	24
−3.0	0	0	0	0	0	0	0	1	2	3	6	10	14	22	27	30	33
−2.7	0	0	0	0	0	0	0	1	2	4	8	13	19	29	36	40	43
−2.3	0	0	0	0	0	0	1	2	3	6	12	18	28	43	53	59	63
−2.0	0	0	0	0	0	0	1	2	4	8	16	25	37	58	71	79	85
−1.7	0	0	0	0	0	0	1	3	6	11	22	34	52	81	99	110	119
−1.3	0	0	0	0	0	1	2	5	10	18	35	56	84	130	160	178	192
−1.0	0	0	0	0	0	1	3	8	15	26	51	81	122	189	233	260	280
−0.7	0	0	0	0	1	2	4	11	21	37	72	114	172	267	329	368	398
−0.3	0	0	0	0	1	3	6	17	32	55	107	168	253	392	484	543	588
0.0	0	0	0	0	1	3	8	22	40	69	133	209	316	489	605	680	737
0.3	0	0	0	0	2	4	10	26	48	83	159	250	377	584	723	815	885
0.7	0	0	0	0	2	5	13	33	59	101	193	302	455	706	877	990	1080
1.0	0	0	0	0	3	7	15	38	68	114	217	340	511	794	988	1120	1210
1.3	0	0	0	1	3	8	18	44	77	128	243	380	571	886	1100	1250	1360
1.7	0	0	0	1	4	10	22	52	90	149	278	434	650	1010	1260	1420	1540
2.0	0	0	0	1	5	12	26	59	100	164	306	474	709	1100	1370	1550	1680
2.3	0	0	0	1	6	15	30	66	111	181	333	515	767	1190	1480	1680	1830
2.7	0	0	0	1	7	17	35	76	125	202	369	568	844	1300	1630	1850	2010
3.0	0	0	1	1	8	20	39	83	135	217	395	605	898	1390	1740	1980	2141
3.3	0	0	1	2	9	21	42	89	145	231	418	639	948	1460	1840	2090	2260

TABLE 5. H_2O-CO_2 overlap correction quantity, $\Delta\epsilon$, for −10C. To obtain $\Delta\epsilon$, multiply values in table by 10^{-4}.

	Log u															
Log h	−3.7	−3.0	−3.0	−2.7	−2.3	−2.0	−1.7	−1.3	−1.0	−0.7	−0.3	0.0	0.3	0.7	1.0	1.3	1.7
−4.0	0	0	0	0	0	0	0	1	1	2	3	4	6	9	10	11	11
−3.7	0	0	0	0	0	0	0	1	2	2	4	6	9	13	15	16	16
−3.3	0	0	0	0	0	0	1	2	2	4	7	10	14	19	23	25	26
−3.0	0	0	0	0	0	0	1	2	3	5	9	13	18	26	31	33	34
−2.7	0	0	0	0	0	1	1	3	4	7	12	17	24	35	41	44	46
−2.3	0	0	0	0	0	1	2	4	7	10	17	25	36	51	60	65	68
−2.0	0	0	0	0	0	1	3	6	9	14	23	34	48	69	81	87	91
−1.7	0	0	0	0	1	2	4	8	12	19	33	48	67	96	113	122	128
−1.3	0	0	0	0	1	3	6	13	20	31	53	78	109	156	183	199	208
−1.0	0	0	0	0	2	4	9	19	30	46	78	114	160	227	267	290	304
−0.7	0	0	0	0	3	6	13	27	42	65	110	161	226	322	380	413	432
−0.3	0	0	0	1	4	10	19	40	63	96	164	239	335	478	564	614	643
0.0	0	0	0	1	5	13	25	50	79	121	206	300	421	600	709	773	810
0.3	0	0	0	1	7	16	30	61	96	146	248	360	505	722	854	932	978
0.7	0	0	1	2	9	20	38	75	117	179	303	440	617	882	1050	1140	1200
1.0	0	0	1	3	11	24	43	86	133	203	343	498	697	998	1180	1300	1360
1.3	0	0	1	3	13	28	50	97	150	228	385	558	781	1120	1330	1460	1520
1.7	0	0	1	4	16	33	59	113	174	262	441	637	890	1270	1520	1660	1740
2.0	0	0	2	5	19	38	66	125	191	288	483	696	971	1390	1650	1820	1900
2.3	0	0	2	6	22	43	73	137	209	314	525	754	1050	1500	1790	1960	2050
2.7	0	1	3	8	26	49	82	152	231	346	577	827	1150	1640	1960	2160	2250
3.0	0	1	3	9	28	53	89	163	246	368	612	876	1220	1740	2080	2290	2390
3.3	0	1	3	10	31	57	95	173	260	388	644	922	1280	1830	2190	2410	2520

emissivities of H_2O and CO_2. Tables 3, 4, 5 and 6 show $\Delta\epsilon$ as a function of u,h at $T=-70$, -40, -10 and 20C. At all temperatures, $\Delta\epsilon$ increases with both u and h. For fixed u,h, comparison of the four tables shows that $\Delta\epsilon$ increases with temperature. This effect traces physically to the increase of the generalized absorption coefficient L with temperature in the wings of both the rotational band of H_2O and the 15 μ CO_2 band. The overlap correction, $-\Delta\epsilon$, for typical total H_2O and CO_2 optical depths, is of the order of -0.05 to -0.10.

6. Ozone emissivity

Ozone emissivity as a function of temperature and optical depth is shown in Fig. 5 and Table 7. The percentage variation with temperature is very large, indicating that the computation of O_3 flux density by means of isothermal emissivities would be subject to large errors if temperature in the vertical column varies substantially. The maximum observed total O_3 is about 0.45 cm, and the corresponding O_3 flux emissivity is about 0.07 for 20C.

TABLE 6. H_2O-CO_2 overlap correction quantity, $\Delta\epsilon$, for 20C. To obtain $\Delta\epsilon$, multiply values in table by 10^{-4}.

	Log u															
Log h	−3.7	−3.3	−3.0	−2.7	−2.3	−2.0	−1.7	−1.3	−1.0	−0.7	−0.3	0.0	0.3	0.7	1.0	1.3	1.7
−4.0	0	0	0	0	0	0	1	1	2	2	4	5	7	9	10	11	11
−3.7	0	0	0	0	0	0	1	2	2	3	5	8	10	13	15	16	16
−3.3	0	0	0	0	0	1	1	2	4	5	8	12	16	21	23	24	25
−3.0	0	0	0	0	0	1	2	3	5	7	11	16	21	28	31	33	34
−2.7	0	0	0	0	1	1	2	4	7	9	15	21	28	37	42	44	45
−2.3	0	0	0	0	1	2	4	7	10	14	23	31	42	55	62	66	67
−2.0	0	0	0	0	1	3	5	9	13	19	31	42	56	75	84	89	91
−1.7	0	0	0	1	2	4	7	13	18	27	43	59	79	104	118	124	127
−1.3	0	0	0	1	3	7	11	20	30	44	70	96	128	170	192	202	207
−1.0	0	0	0	1	5	10	17	30	44	64	102	141	187	248	281	296	303
−0.7	0	0	1	2	7	14	24	43	63	91	145	201	266	354	400	423	432
−0.3	0	0	1	3	11	21	36	64	94	136	217	299	397	528	598	633	647
0.0	0	0	1	5	14	27	46	81	119	172	274	378	502	668	758	803	821
0.3	0	0	2	6	18	33	56	99	145	209	332	458	608	810	920	975	997
0.7	0	1	3	8	23	42	69	122	180	259	410	564	748	998	1140	1200	1230
1.0	0	1	3	10	27	49	79	140	205	295	467	641	849	1130	1290	1370	1400
1.3	0	1	4	12	32	55	90	158	231	332	524	719	952	1270	1450	1540	1580
1.7	0	2	5	15	38	65	104	181	266	381	600	820	1080	1450	1660	1760	1800
2.0	0	2	7	17	42	72	115	199	291	417	654	893	1180	1580	1800	1920	1970
2.3	0	3	8	19	47	79	125	216	315	451	706	962	1270	1700	1940	2070	2120
2.7	0	3	9	22	53	88	138	237	345	493	770	1050	1380	1850	2120	2270	2320
3.0	0	4	10	24	57	94	147	251	365	521	813	1110	1460	1950	2240	2400	2460
3.3	1	4	12	27	61	100	155	265	385	549	855	1160	1530	2050	2360	2520	2590

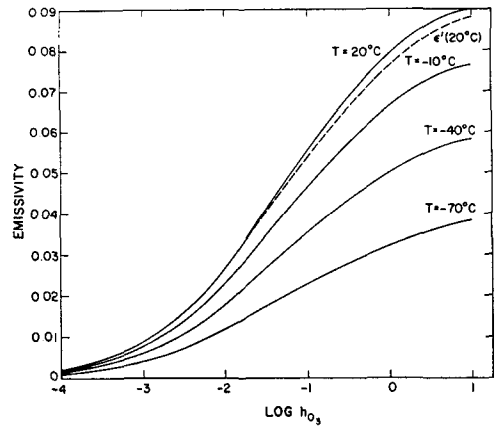

FIG. 5. O_3 emissivity as a function of optical depth (pressure-corrected cm at STP) for $T=20$ and -70C, and the incorrect emissivity ϵ' for $T=20$C.

TABLE 7. Flux emissivities for O_3 (percent).

Log h_{O_3}	−70C	−40C	−10C	20C
−4.0	0.109	0.155	0.191	0.214
−3.7	0.167	0.239	0.300	0.340
−3.3	0.284	0.412	0.520	0.594
−3.0	0.415	0.610	0.777	0.896
−2.7	0.588	0.872	1.12	1.29
−2.3	0.900	1.34	1.72	1.99
−2.0	1.20	1.79	2.30	2.68
−1.7	1.53	2.31	2.99	3.51
−1.3	1.99	3.03	3.97	4.71
−1.0	2.30	3.54	4.66	5.55
−0.7	2.59	4.01	5.30	6.33
−0.3	2.97	4.60	6.10	7.29
0.0	3.24	5.02	6.64	7.93
0.3	3.47	5.36	7.08	8.43
0.7	3.71	5.68	7.47	8.84
1.0	3.83	5.84	7.65	9.03

7. Concluding remarks

The emissivities calculated here apply to an atmosphere at standard pressure and various isothermal temperatures. The emissivities are those actually implied by Elsasser's (1960) treatment of the basic absorption data available at that time and correct emissivities previously based on the Elsasser monograph but flawed by a mathematical error. The separate contributions of the three spectral regions of H_2O have been presented in order to facilitate meaningful comparisons with other work.

An important remaining source of error in the emissivities presented here traces to Elsasser's treatment of the dependence of absorption coefficients on temperature. A minor part of this error results from classical as opposed to quantum mechanical treatment of the partition function, but the major part results from application of the temperature correction for a single absorption line to the generalized absorption coefficient for a band. The error is analogous to the error that results from applying the pressure scaling of optical depth, valid for a single line, to an entire band. The error in temperature dependence is essentially eliminated in transmissivity data calculated from a quasi-random model by Wyatt *et al.* (1962), in which the temperature dependence is applied to lines within small spectral and intensity intervals. Their results for standard pressure and temperature differ somewhat, of course, from those of Elsasser. The limiting factor in their results appears to be the accuracy of the experimentally derived line intensities. Jurica (1970) has calculated emissivities from the data of Wyatt *et al.* and others. Significant differences between these presumably more accurate emissivities and those implied by Elsasser's treatment were found, but discussion goes beyond the scope of this paper.

The H_2O emissivities ϵ calculated here exceed the erroneous ϵ' by 10–15% at the higher temperatures over a wide range of optical depths. It follows that the use of ϵ' underestimates downward flux density at the surface by 10–15%. The errors in upward and net upward radiation are more difficult to analyze without making actual computations; however, it appears that use of ϵ' overestimates the net upward H_2O radiation at the top of the atmosphere, as well as at the surface, but more so at the surface. Thus, the cooling rate, which depends on the gradient of the net radiation, would be underestimated by use of ϵ'. These inferences are consistent with recent calculations of downward flux density and cooling by Sasamori (1968). He found that use of Elsasser's radiation tables led to downward flux densities and cooling rates which were of the order of 15% smaller than observations and certain calculations based on other methods. However, the comparison cannot be pushed very far, since the contributions by O_3, CO_2 and by overlap were not discussed by Sasamori, and observations of downward flux density presently available are subject to errors of the order of the discrepancies between the various calculations. In addition, it is not entirely clear that the error in Elsasser's tabulations leads ultimately to precisely the same consequences in terms of net radiation and cooling rates as does the error in emissivity. Moreover, the use of laboratory emissivities for homogeneous paths can introduce sizable errors (Rodgers, 1967). A careful assessment of the errors in the use of Elsasser's tables seems called for, but goes beyond the scope of this paper.

Acknowledgment. The research reported in this paper has been supported by the Office of Naval Research under Contract Nonr N 00014-67-A-0209-0004.

REFERENCES

Brooks, D. L., 1950: A tabular method for the computation of temperature change by infrared radiation in the free atmosphere. *J. Meteor.*, **7**, 313–321.

Elsasser, W. M., with M. F. Culbertson, 1960: Atmospheric radiation tables. *Meteor. Monogr.*, **4**, No. 23, 1–43.

Fleagle, R. G., and J. A. Businger, 1963: *An Introduction to Atmospheric Physics*. New York, Academic Press, 346 pp.

Jurica, G. M., 1970: Radiative flux densities and heating rates in the atmosphere using pressure and temperature-dependent emissivities. Ph.D. dissertation, University of Arizona.

Rodgers, C. D., 1967: The use of emissivity in atmospheric radiation calculations. *Quart. J. Roy. Meteor. Soc.*, **93**, 43–54.

Sasamori, T., 1968: The radiative cooling calculation for application to general circulation experiments. *J. Appl. Meteor.*, **7**, 721–729.

Sellers, W. D., 1965: *Physical Climatology*. The University of Chicago Press, 272 pp.

Wyatt, P. J., V. R. Stull and G. N. Plass, 1962: The infrared absorption of water vapor. Infrared transmission studies, Final Rept. SSD-TDR-62-127, Vol. II, Aeronutronic Div., Ford Motor Co., 249 pp.

Zdunkowski, W. G., R. E. Barth and F. A. Lombardo, 1966: Discussion on the atmospheric radiation tables by Elsasser and Culbertson. *Pure Appl. Geophys.*, **63**, 211–219.